Semiclassical Wave Packet Treatment of Scattering Resonances: Application to the Delta Zero-Point Energy Effect in Recombination Reactions

Evgeny Vetoshkin and Dmitri Babikov*

Chemistry Department, Marquette University, Milwaukee, Wisconsin 53201, USA

(Received 12 April 2007; published 24 September 2007)

For the first time Feshbach-type resonances important in recombination reactions are characterized using the semiclassical wave packet method. This approximation allows us to determine the energies, lifetimes, and wave functions of the resonances and also to observe a very interesting correlation between them. Most important is that this approach permits description of a quantum delta–zero-point energy effect in recombination reactions and reproduces the anomalous rates of ozone formation.

DOI: 10.1103/PhysRevLett.99.138301 PACS numbers: 82.20.−w, 34.10.+x, 34.30.+h, 34.50.−s

In recent years there has been an increased interest in the theoretical treatment of multibody recombination reactions. These processes represent examples where, due to the importance of several quantum effects, the Schrödinger equation should be employed in order to treat the motion of nuclei in the course of the chemical transformation. The first quantum feature is brought by scattering resonances which play the role of the metastable intermediate species. For example, the ozone forming reaction proceeds through formation of metastable O_3^* states that are subsequently stabilized by collisions with bath gas molecules:

$$O + O_2 \rightleftarrows O_3^* \rightleftarrows O_2 + O, \tag{1a}$$

$$O_3^* + M \rightarrow O_3 + M. \tag{1b}$$

When different isotopes of oxygen are involved the difference of vibrational zero-point energies (ΔZPE) of the fragments on the left- and right-hand sides of reaction (1a) gives rise to the second quantum effect—it was shown that scattering resonances within this ΔZPE range are energetically accessible only from the lower entrance channel, which increases recombination rates by as much as 60% [1] and leads to the anomalously large isotope effect observed in ozone [2]. The third effect is quantum symmetry, which can reduce the recombination rates by 10% to 15% [3]. Note that the classical trajectory simulations or statistical theory only mimic these effects by empirically introducing *ad hoc* corrections [4,5] while the fully quantum treatment of the continuum states is very demanding. Although previous authors have recognized the importance of quantum effects, the studies reported to date [1,6,7] have been restricted to various approximations and have not achieved a complete solution of the problem. This is why the remarkable anomalous isotope effect discovered 25 years ago in ozone [8,9] is not yet fully understood [10]. Similar isotope effects are found in NO_2, S_3, and SO_2 and it is reasonable to assume that symmetry, resonances, and ΔZPE, all three being general quantum effects, are responsible for those anomalies as well.

In this Letter we propose a new theoretical approach to recombination reactions which includes all quantum effects and is very affordable computationally. For the first time we apply the semiclassical initial value representation (IVR) method [11] to treat Feshbach-type resonances participating in recombination, particularly those in the vicinity of the ΔZPE energy range. We demonstrate that this method permits us to capture the quantum ΔZPE effect and even to obtain the associated anomalous isotope effect. Our approach is general and can be applied to a variety of reactions.

Since the ΔZPE is essentially a multichannel effect, the simplest potential energy surface (PES) suitable for a proof-of-principle study must have two equivalent entrance or exit channels. For example, there are two channels associated with population and decay of the metastable states of an asymmetric ozone isomer: $^{16}O + {}^{16}O^{18}O \leftrightarrow ({}^{16}O^{16}O^{18}O)^* \leftrightarrow {}^{16}O^{16}O + {}^{18}O$. Therefore, for this work we constructed an analytic two-dimensional PES $V(r_1, r_2)$ using two coupled Morse oscillator functions. This surface only mimics the major features of ozone PES [1] such as dissociation energy, frequencies at the bottom of the well and in the channels. Other than that, the shape of our PES is general and is quite typical to many barrierless recombination reactions (see Fig. 1 and EPAPS material [12]). The deep covalent bonding well gives rise to a progression of long-lived scattering resonances and we use the semiclassical IVR method to determine their energies, lifetimes, and wave functions.

In the semiclassical IVR method the initial wave packet $\psi(\mathbf{r}, 0)$ is expanded over an overcomplete set of N Gaussian functions placed at randomly chosen initial points $(\mathbf{r}_i, \mathbf{p}_i)$ in the phase space, and the time evolution of the wave function $\psi(\mathbf{r}, t)$ is approximated by an integral over this initial phase space. The N independent trajectories are propagated in a usual classical way from $(\mathbf{r}_i, \mathbf{p}_i)$ to $(\mathbf{r}_t, \mathbf{p}_t)$ at time t. In addition, the phase $S(t)$ and the complex preexponential factor $C(t)$ are integrated along each trajectory [11], which allows different trajectories to interfere and contribute coherently into the overall wave function. All quantum mechanical effects arise as a result of this interference. For simplicity, the initial wave packet $\psi(\mathbf{r}, 0)$ can be chosen as a Gaussian function centered at some point $\mathbf{r}_0$ and characterized by some width parameter

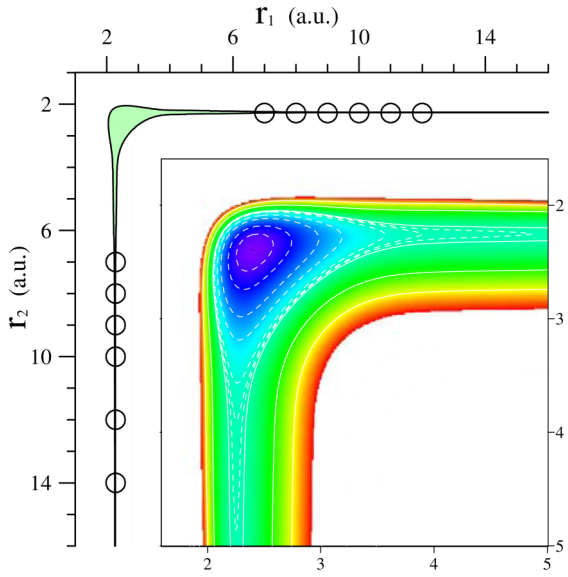

FIG. 1 (color online). Two views of the potential energy surface used here to study recombination. The well depth is 1.13 eV. The shaded area shows configuration space below the classical dissociation limit $E = 0$. Circles represent the initial wave packets.

α. In this case $\psi(\mathbf{r}, t)$ is calculated as a sum of analytical expressions [13]. However, for accurate description of the metastable states the values of $\mathbf{r}_0$ and α must be carefully chosen in order to narrow the energy spectrum and maximize overlap with scattering wave functions. We found that in order to capture the metastable states in a barrierless potential the best position for the initial wave packet is far in the channel, as shown in Fig. 1. The width should be comparable to the expected internodal distance. We also found that propagation of several wave packets is usually required in order to describe all the states in a broad energy range. Note that wave packets placed in the well region of the PES capture mostly the bound vibrational states.

The major difficulty of the semiclassical IVR approach is associated with appearance of chaotic (unstable) trajectories. For such trajectories the prefactor $C(t)$ becomes exponentially large, which leads to poor convergence with respect to N and reduces accuracy. This is particularly the case for multidimensional potentials and at long propagation times, both specific to our system. Here, even with $N = 10^7$ the propagation time was limited by the chaotic behavior to only $t \sim 0.3$–0.4 ps, which is insufficient for spectral analysis. To overcome this problem it was suggested to monitor the values of $C(t)$ and remove any trajectory if its prefactor exceeds a chosen cutoff value [14]. Following this procedure we lost up to 15% of trajectories, which is highly undesirable at long propagation times when the sampling is already deteriorated by the wave packet spreading. We adopted a better approach. Since our primarily purpose is to calculate the autocorrelation function $P(t) = \langle\psi(\mathbf{r}, 0)|\psi(\mathbf{r}, t)\rangle$ we should remove trajectories only based on the value of the product of prefactor $C(t)$ and exponential factor for overlapping Gaussian functions (see Eq. (20) in Ref. [13]). This new cutoff procedure allowed us to extend the propagation time to ~3–4 ps (i.e., by an order of magnitude) keeping the amount of deleted trajectories at only 0.5%. Figure 2 gives an example of the autocorrelation function calculated using our cutoff procedure for a typical initial wave packet. For comparison we propagated the same wave packet using the fully quantum Chebyshev method and the quantum and semiclassical autocorrelation functions agree well during the initial 0.6 ps, after which the quantum method requires a significant extension of the grid (due to fast motion of the wave packet into the channels) and becomes computationally impractical at ~1 ps. Note that the semiclassical method allows us to continue propagation without increase in the computational cost. In terms of the CPU time the semiclassical IVR was about 4 times faster. Another important feature of the IVR is its intrinsic massive parallelization. The N trajectories are totally independent and can be distributed among different processors and propagated in parallel without any message passing which gives a tremendous advantage in terms of the wall clock time. For example, we run our calculations using 1024 processors of the *Seaborg* machine at NERSC and achieved acceleration by another factor of 10^3 compared to one-processor quantum propagation.

Energies E_n and widths Γ_n of the scattering resonances were extracted from the autocorrelation function using the Prony method [15]. This approach fits $P(t)$ obtained on a grid of time points by a function $P(t) = \sum_{n=1}^{L} b_n \exp\{-i(E_n - i\Gamma_n/2)t\}$ where the b_n are probability amplitudes. Each autocorrelation function was analyzed several times trying different values of L. The uncertainty of each E_n and Γ_n was estimated as its deviation from an average value when L is varied. For the $^{16}O^{16}O^{18}O$ isomer of ozone the ΔZPE part of spectrum extends from 839.4 to 863.4 cm^{-1}; our results for the vicinity of this region are given in Table I. For the bound

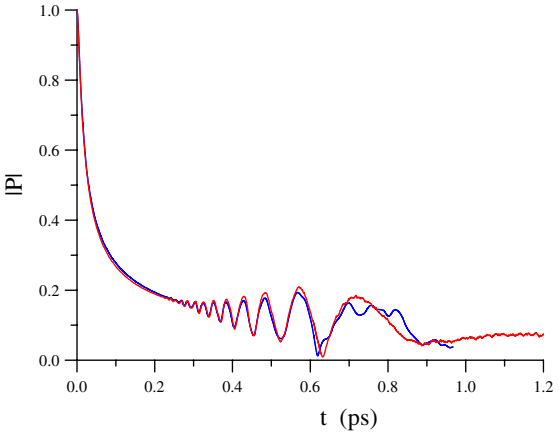

FIG. 2 (color online). The autocorrelation function obtained from semiclassical (blue or dark gray) and quantum (red or gray) propagation of a Gaussian wave packet with $\alpha = 50$, $r_1 = 9.0$ a.u. and $r_2 = 2.28$ a.u.

TABLE I. Energies and widths of bound and metastable states of $^{16}O^{16}O^{18}O$ in the vicinity of the ΔZPE energy range using 2D potential from Fig. 1. These data were obtained via Prony analysis of autocorrelation functions found from the semiclassical propagation of wave packets.

	Open channel		Closed channel	
	$E(\mathrm{cm}^{-1})$	$\Gamma(\mathrm{cm}^{-1})$	$E(\mathrm{cm}^{-1})$	$\Gamma(\mathrm{cm}^{-1})$
Metastable states above the ZPE of $^{16}O^{16}O$	899.3	325.0	894.5	101.0
	885.6	135.0	891.3	58.0
	872.7	100.0	881.6	42.0
	865.4	66.0	875.1	27.0
			865.5	16.0
Metastable states within the ΔZPE region	861.4	40.0	861.4	0.06±0.03
	857.4	36.0	858.2	0.06±0.04
	845.3	26.5	850.9	0.06±0.04
	841.2	15.0	840.4	0.06±0.05
Bound states below the ZPE of $^{16}O^{18}O$	837.2		835.6	
	825.8		817.0	
	807.3		788.0	
	784.7			

states (below ΔZPE) the uncertainties of E_n are within 0.2 cm^{-1}. For scattering resonances in the ΔZPE range the uncertainties are about 0.4 cm^{-1} while for upper resonances near 900 cm^{-1} they reach ~1 cm^{-1}. The uncertainties associated with widths are somewhat larger and depend on state character. Thus, for broader resonances the uncertainty of Γ_n is usually less then 10% of its value and ranges from 1.5 to 30 cm^{-1}. Note that within the ΔZPE range there are several very narrow (sub-wave-number) resonances and determination of accurate Γ_n for those is not simple. One way to improve precision is to obtain (from the first propagation of Gaussian wave packet) the eigenfunction and to repeat propagation using it as a better initial function $\psi(\mathbf{r}, 0)$. This approach allowed us to narrow the range of uncertainty for widths of these states down to about 0.05 cm^{-1}, which corresponds to lifetimes on the order of $\tau \approx 100$ ps. Further improvement is still desirable and in future work we plan to replace the Prony method by another method of analysis of $P(t)$, that would be less sensitive to the noise which appears in the IVR autocorrelation function at $t > 0.8$ ps (see Fig. 2).

When energies E_n are known the wave functions of the metastable states can be found as Fourier transform of the propagated wave packets. Analysis of wave functions shows a very clear correlation between the nature of states and their lifetimes. First of all, we found that the majority of the metastable states exhibit *local vibration mode* character, either $^{16}O^{16}O - {}^{18}O$ or $^{16}O - {}^{16}O^{18}O$, and are localized almost entirely in only one channel. Figures 3 and 4(a) show wave functions for two such states, both within the ΔZPE range. In either case the number of quanta along one channel is $n = 22$ and is zero along the other channel. The energy difference between these states is only 4 cm^{-1} but their lifetimes are very different: 90.0 and 0.15 ps,

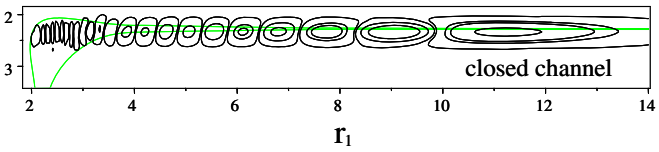

FIG. 3 (color online). Modulus of the wave function for a metastable state at $E = 861.4$ cm^{-1} obtained from semiclassical propagation given in Fig. 2. The wave function is entirely localized in the closed channel and the lifetime is very large.

respectively. The reason becomes clear if we recall that within the ΔZPE range only the channel giving $^{16}O + {}^{16}O^{18}O$ is energetically open [due to lower zero-point energy (ZPE) of the $^{16}O^{18}O$ product] while the $^{16}O^{16}O + {}^{18}O$ channel is still closed. Because the state of Fig. 4 is localized in the open channel it decays faster, while the state of Fig. 3 is localized in the closed channel and should "flow" through the interaction region in order to reach the channel open for decay. This interesting property is an important finding of this Letter and is an example of a mode specific decay [16]. The resonances in this problem occur due to interaction of two local vibration modes, $^{16}O^{16}O + {}^{18}O$ and $^{16}O + {}^{16}O^{18}O$. (Indeed, the wave func-

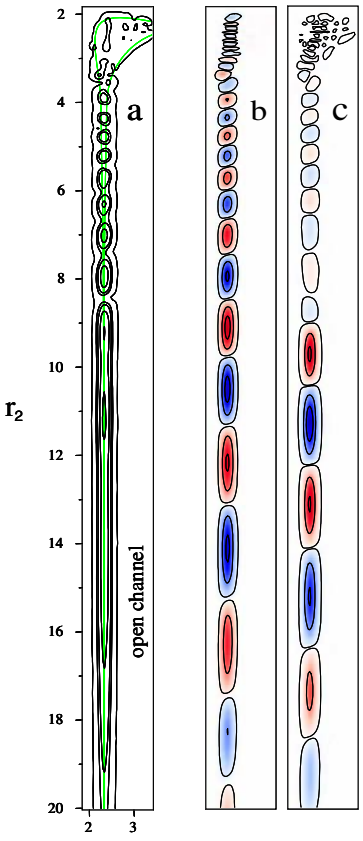

FIG. 4 (color online). (a) Modulus, (b) real, and (c) imaginary part of the wave function for the metastable state at $E = 857.4$ cm^{-1} obtained from semiclassical propagation of a Gaussian wave packet with $\alpha = 50$, $r_1 = 2.28$ a.u., and $r_2 = 9.0$ a.u. The wave function is entirely localized in the open channel and the lifetime is short.

tion in Fig. 4 is not purely one-dimensional; it exhibits some probability in the well region and towards the other channel, especially its imaginary part). Furthermore, all the narrow resonances in the ΔZPE range can be viewed as Feshbach resonances since the entrance open channel ($^{16}O + {}^{16}O^{18}O$) interacts with another channel of the PES which is closed ($^{16}O^{16}O + {}^{18}O$). Such states are very different from the shape resonances trapped by a centrifugal barrier [13].

The wave functions for other states in Table I look very similar to those in Figs. 3 and 4 and can be attributed to one or the other progression. (One exception is a hyperspherical state [16] at 891.3 cm^{-1} which is about symmetric.) Note that above the ΔZPE range the two progressions of the local vibration states continue, but their lifetimes become comparable since both channels are open at these energies. The wave functions of long-lived states, like the one in Fig. 3, are basically real valued, while the wave functions of fast-decaying states exhibit a non-negligible imaginary part, as shown in Figs. 4(b) and 4(c).

To model the kinetics we consider the processes of formation, decay, and stabilization of the metastable states. Lifetimes define the decay rates; formation rates are obtained from the equilibrium condition for reaction (1a); stabilization rates are calculated using the "exponential down" model $k^s_{nm} \sim \exp\{-(E_n - E_m)/\Delta E\}$ with $\Delta E = 20.0\ cm^{-1}$. We include stabilizing transitions $n \rightarrow m$ from every metastable state into all other metastable and several upper bound states within each progression. Details of this treatment will be given elsewhere. The same isotopomer $^{16}O^{16}O^{18}O$ can be formed from the two channels and we focus on ratio of the rate coefficients $R = k_{18+1616}/k_{16+1618}$. The metastable states *above* the ΔZPE range are energetically accessible from both channels and overall they contribute about equally to $k_{18+1616}$ and $k_{16+1618}$. Here each localized state is associated with its channel while the contribution of a symmetric state is split. The anomalous isotope effect ($\mathcal{R} < 1$) appears because the states within the ΔZPE range can be populated only from one channel, $^{16}O + {}^{16}O^{18}O$, and when stabilized they contribute exclusively to this channel of reaction, regardless of their vibrational character. The resultant effect is significant but we found that the uncertainty of the Γ_n values for narrow resonances in the ΔZPE range leads to some uncertainty in the magnitude of the effect. Thus, if for those narrow states we take the upper values of Γ_n (see Table I) the isotope effect we observe is $\mathcal{R} = 0.36$. Taking the lower values for every such Γ_n we obtain $\mathcal{R} = 0.72$. The experimental value for ozone, $\mathcal{R}_{exp} = 0.63$ [2], falls into this range and is closer to the second case. It is also important to mention that within our model there are two limiting cases when the actual values of Γ_n become unimportant. The limit of very narrow resonances $\Gamma_n \ll k^s_{nm}[M]$ is achieved when $\Gamma_n < 0.003\ cm^{-1}$ ($\tau > 2$ ns). Narrow resonances do not receive any population from the open channel and basically behave like the bound states in the closed channel, which makes this isotope effect disappear. In the opposite limit ($\Gamma_n \gg k^s_{nm}[M]$, achieved when $\Gamma_n > 0.4\ cm^{-1}$ or $\tau < 13$ ps) the isotope effect is at a maximum and gives $\mathcal{R} = 0.15$.

In this Letter we applied the semiclassical IVR approach to fully characterize scattering resonances in a recombination reaction. Our approach is computationally affordable and highly parallel; it captures the ΔZPE effect and reproduces the anomalous isotope effect. Here we used oxygen masses and the PES similar to ozone just because ozone is well studied experimentally, but the method is general and can be used for a variety of reactions. We found that wave functions of the metastable states are localized in one of the channels (either open or closed) which explains the pattern of lifetimes. The anomalously large isotope effect is due to Feshbach-type resonances in the ΔZPE range. The magnitude of the effect is determined by their lifetimes and (in a general limiting case) can reach 85% of the rate.

This research was supported by the Petroleum Research Fund, Grant No. 43298-G6. We used computational resources of the NERSC Center, supported by the DOE Office of Science under Contract No. DE-AC03-76SF00098.

*Corresponding author.
dmitri.babikov@mu.edu

[1] D. Babikov, B. K. Kendrick, R. B. Walker, P. Fleurat-Lessard, R. Schinke, and R. T Pack, J. Chem. Phys. **118**, 6298 (2003); **119**, 2577 (2003); Chem. Phys. Lett. **372**, 686 (2003).
[2] C. Janssen, J. Guenter, K. Mauersberger, and D. Krankowsky, Phys. Chem. Chem. Phys. **3**, 4718 (2001).
[3] R. T Pack, R. B. Walker, and B. K. Kendrick, J. Chem. Phys. **121**, 800 (2004).
[4] R. Schinke and P. Fleurat-Lessard, J. Chem. Phys. **122**, 094317 (2005).
[5] Y. Q. Gao and R. A. Marcus, Science **293**, 259 (2001).
[6] T. Xie and J. M. Bowman, Chem. Phys. Lett. **412**, 131 (2005).
[7] D. Charlo and D. C. Clary, J. Chem. Phys. **120**, 2700 (2004).
[8] K. Mauersberger, Geophys. Res. Lett. **8**, 935 (1981).
[9] M. H. Thiemens and J. E. Heidenreich III, Science **219**, 1073 (1983).
[10] K. Luther, K. Oum, and J. Troe, Phys. Chem. Chem. Phys. **7**, 2764 (2005).
[11] M. F. Herman and E. Kluk, Chem. Phys. **91**, 27 (1984).
[12] See EPAPS Document No. E-PRLTAO-99-007739 for a FORTRAN code to generate the values of energy, gradients and Hessians for the potential energy surface used in this work. For more information on EPAPS, see http://www.aip.org/pubservs/epaps.html.
[13] E. Vetoshkin and D. Babikov, J. Chem. Phys. **125**, 024302 (2006).
[14] K. G. Kay, J. Chem. Phys. **101**, 2250 (1994).
[15] S. K. Gray, J. Chem. Phys. **96**, 6543 (1992).
[16] S. Y. Lin, H. Guo, and S. C. Farantos, J. Chem. Phys. **122**, 124308 (2005).